Research Square

Preprints are preliminary reports that have not undergone peer review.
They should not be considered conclusive, used to inform clinical practice,
or referenced by the media as validated information.

Design and Simulation of a Tunable Meta-surface Filter Based on Liquid Crystal in the VIS–NIR Wavelength Range

KHASHAYAR MOKHTARI NASR
Imam Hossein University (IHU)
EBRAHIM HAJIALI
Imam Hossein University (IHU)
ALI SHEKARI
a_shekari@ihu.ac.ir

Imam Hossein University (IHU)

Article

Keywords:

Posted Date: July 24th, 2026

DOI: https://doi.org/10.21203/rs.3.rs-9876004/v1

License: This work is licensed under a Creative Commons Attribution 4.0 International License.
Read Full License

Additional Declarations: No competing interests reported.

Design and Simulation of a Tunable Meta-surface Filter Based on Liquid Crystal in the VIS–NIR Wavelength Range

KHASHAYAR MOKHTARI NASR,[1, †] EBRAHIM HAJI ALI,[2, *] AND ALI SHEKARI [3, †]

[1] *M.Sc., Department of Physics, Faculty of Science, Imam Hossein University (IHU), Tehran, Iran.*
[2] *Assistant Professor, Department of Physics, Faculty of Science, Imam Hossein University (IHU), Tehran, Iran.*
[3] *Researcher, Faculty of Materials, Imam Hossein University (IHU), Tehran, Iran.*
[†] *These authors contributed equally.*
**a_shekari@ihu.ac.ir*

Abstract: This study introduces a tunable optical filter based on a 1D aluminum metasurface combined with nematic liquid crystal (E7) for the VIS–NIR range. Using COMSOL simulations, the design exploits the liquid crystal's birefringence and electro-optical properties to enable voltage-controlled tuning without physical alteration. Structures with varying grating periodicities were tested under TE and TM polarizations. Results show that TM polarization and double-layer configurations yield sharper resonances. Liquid crystal integration causes red shifts in peaks, offering dynamic reconfigurability. The findings highlight the design's applicability in adaptive filters, optical sensors, and photonic switching.

1. Introduction

In recent decades, optical and photonic technologies have made remarkable advancements and found extensive applications in various fields such as medical imaging, optical communications, remote sensing, military industries, precision agriculture, and sensor systems. Among these, optical filters play a crucial role as key components in the separation and control of specific light wavelengths. However, traditional optical filters are limited in performance and lack the ability to adapt to changing environmental conditions or variations in input signals [1,2].

To overcome these limitations, research efforts have focused on developing tunable optical filters. In this context, two emerging technologies—liquid crystals and meta-surfaces—have been introduced as effective and complementary options. Liquid crystals, with properties such as birefringence and high sensitivity to electric fields, enable the tuning of the refractive index of the medium. On the other hand, meta-surfaces, composed of periodic nanostructures, possess the ability to precisely control optical properties such as phase and polarization of light. Fig. 1 illustrates a schematic of a tunable optical filter based on these technologies.

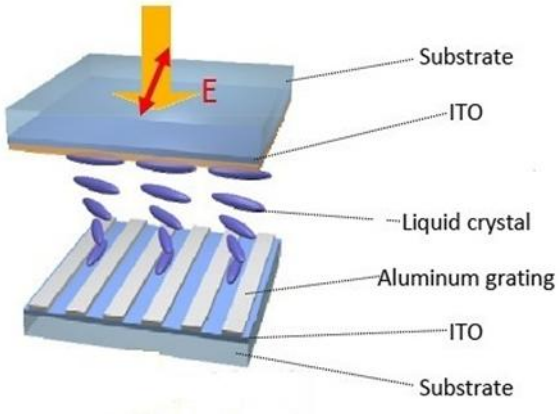


Fig. 1 Schematic of a liquid crystal-based metasurface filter [2]

This study takes an effective step toward the development of a new generation of smart filters by designing and simulating a tunable optical filter based on liquid crystal and metallic meta-surfaces. The proposed structure enables precise control over the transmission spectrum through the application of an electric voltage while maintaining suitable thermal and mechanical stability. Given its high performance and potential for mass production, this filter holds significant promise for commercialization and deployment across various industries. One of the key phenomena in this field is the generation of surface plasmons, during which the energy and momentum of photons incident on a metal surface are transferred to collective oscillations of free electrons. This process leads to the formation of surface electromagnetic waves known as surface plasmons. This excitation typically occurs when p-polarized light is incident on a metallic surface such as gold, interfacing with a low refractive index medium (e.g., gas or liquid) at a specific angle, resulting in a reduction in the intensity of reflected light (Fig. 2).

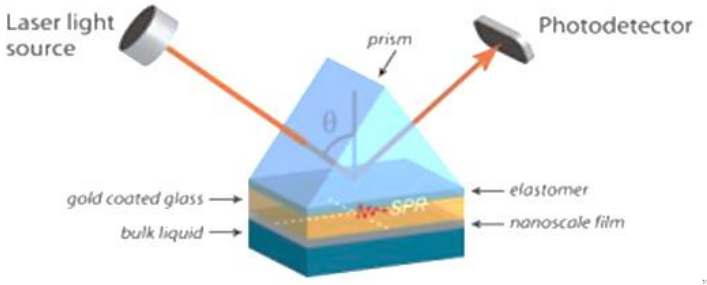


Fig. 2: Surface Plasmon Excitation [3]

In numerous applications, including LCD displays, optical switches, projectors, and mobile phones, liquid crystals are extensively used. Thermotropic liquid crystals, especially their uniaxial types, are highly valuable for designing optical devices due to their anisotropic optical properties and direction-dependent refractive indices. The refractive index tensor structure of these liquid crystals is expressed as follows [4]:

$$n = \begin{bmatrix} n_{\perp} & 0 & 0 \\ 0 & n_{\perp} & 0 \\ 0 & 0 & n_{\parallel} \end{bmatrix} \quad (1)$$

Here, the parallel (∥) and perpendicular (⊥) notations indicate that the molecular axis is aligned either parallel or perpendicular to the optical axis. In optical regions, $\varepsilon_{\perp} = \varepsilon_0 n_0^2, n_{\parallel} = \varepsilon_0 n_e^2$, resulting in $\Delta\varepsilon = \varepsilon_0(n_e^2 - n_0^2)$. The propagation of light at an incident angle θ relative to the optical axis of the liquid crystal is illustrated in Fig. 3 [5].

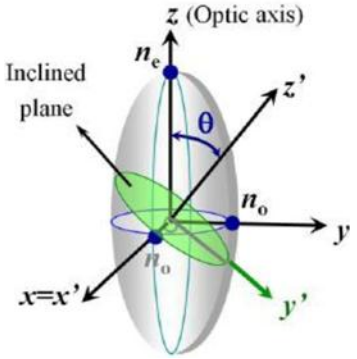


Fig. 3 Light Propagation in a Uniaxial Liquid Crystal Medium [5].

When light is incident on a birefringent material such as a liquid crystal, the electric field vector splits into two mutually orthogonal components aligned along two principal optical axes. Each component experiences a different refractive index corresponding to a distinct propagation mode. One of these modes, which is polarized perpendicular to the plane formed by the wave vector and the optical axis, is called the ordinary wave, and its associated refractive index is referred to as the ordinary refractive index (n_o). It is important to note that n_0 is independent of the angle of incidence (θ). The other mode, whose polarization direction is parallel to the plane formed by the wave vector and the optical axis, is called the extraordinary wave. The refractive index associated with this mode is the extraordinary refractive index (n_e), which depends on the angle of incidence (θ). Therefore, the effective refractive index of the medium can be expressed by the following relation [5].

$$n_{eff}(\theta) = \left[\frac{\cos^2\theta}{n_0^2} + \frac{\sin^2\theta}{n_e^2}\right]^{-1} \quad (2)$$

Optical anisotropy, which fundamentally arises from the anisotropic molecular structure of liquid crystals, plays a crucial role in altering the polarization state of light. Optical anisotropy—or birefringence—is defined as:

$$\Delta n = n_e - n_0 \quad (3)$$

If $n_e > n_0$, the liquid crystal exhibits positive birefringence, meaning the extraordinary wave experiences a greater delay compared to the ordinary wave. Conversely, if $n_e < n_0$, the crystal exhibits negative birefringence, and the birefringence value is typically smaller than that of positive birefringent materials. This behavior directly influences the optical path difference and phase modulation, which are critical for tunable photonic devices. In most liquid crystals, the value of Δ_n is positive, and it is regarded as one of the key parameters in the design of liquid crystal-based optical devices [5].

One of the key innovations of this design is the use of E7 liquid crystal, which offers thermal stability, fast response, and a broad transmission spectrum. In addition, the incorporation of nanostructured aluminum meta-surfaces enhances precision in controlling optical properties. A significant advantage of this filter is that spectral tuning does not require any physical modifications—it can be reconfigured simply by applying an external voltage. These features make the proposed structure highly suitable for the following applications:

- Hyperspectral imaging
- Biological and chemical sensors
- Smart optical fibers
- Airborne and field-deployable optical systems
- Low-power optical communication systems [6,7]

Other prominent features of this filter include its compatibility with industrial technologies such as nanolithography, thermal evaporation, and photopolymerization [8], which enables large-scale production and commercialization. This structure can be utilized in portable devices, medical equipment, agricultural sensors, and low-power communication systems [6,7]. This study, organized into five sections, focuses on the design and simulation of a tunable metasurface filter based on liquid crystal in the visible to near-infrared (VIS-NIR) wavelength range. The first section presents an introduction to the topic and its significance. The second section is dedicated to reviewing the technical literature and previous studies. The third section details the research methodology and the steps involved in the design and simulation process. The fourth section presents the results of the simulations along with their analysis. Finally, the fifth section provides a summary and overall conclusion of the research findings.

2. Literature review

Bohlouli and Chaharmahali (2018) focused their study on the design of microwave and RF band-pass filters using microstrip lines. They achieved improved performance by reducing the filter size and optimizing the frequency passband parameters. Their primary goal was to enhance the characteristics of RF filters and minimize insertion loss [9].

However, Shamizadeh and Alizadeh (2015) took a different approach by designing a tunable optical filter based on ring resonators for optical communication systems. Their design enabled wavelength tuning and reduced crosstalk. Although both studies focus on tunable filters, they differ significantly in terms of technology platform and application context [10]. Shi et al. (2017) also worked in the field of optical filters and successfully developed tunable color filters using aluminum meta-surfaces and nematic liquid crystals. These filters could change color by applying a low voltage. This approach, which is based on metasurface technology, provides more precise tunability and better energy efficiency compared to conventional methods [2]. In contrast, Kao and Lalanne (2002) focused more on the fundamental and theoretical aspects of light transmission through metallic gratings. By demonstrating the negative impact of surface plasmons, they led to a reconsideration of design approaches for such systems. These two approaches are entirely different—one is application-oriented and tunable, while the other is fundamental and critical [11]. Palto et al. (2016), with an emphasis on the application of nematic liquid crystals, designed a composite structure capable of controlling light transmission through applied voltage while achieving faster response times. They demonstrated that two electro-optic effects exist within this structure, enabling more efficient tuning of its optical behavior [8]. This subject was further developed by Yu et al. (2024), who designed a narrowband filter with an ultra-high quality factor and precise wavelength tunability, making it highly suitable for sensitive telecommunication applications [12]. Shen et al. (2021) also explored the use of tunable all-dielectric meta-surfaces for data security, demonstrating that nematic liquid crystals can enable flexible encryption and decryption processes. This application shifts the focus from filtering and tunability, emphasized in previous studies, to the security aspects of optical technologies [13]. Finally, Mirbagheri and Karooz (2022) adopted a different approach by utilizing thermal variations to tune optical metamaterials. Their method provides a non-electrical, temperature-based solution for controlling modes and spectral responses [14].

Overall, despite their technological and application-based differences, all the studies aim to advance tunable optical filters and structures. Some researchers, such as Bahlouli and Chaharmahali, have primarily focused on RF and microstrip filters, while others, like Shi and Yu, have employed metasurface technology and nematic liquid crystals to achieve more precise wavelength tuning and light transmission control. Still, others, such as Kao and Lalan, have addressed fundamental issues and refined conceptual frameworks, while groups like Shen and Mirbagheri have introduced novel applications in data security and temperature-based tuning. These differences reflect the diversity of approaches and the broad range of technologies utilized in this field.

In other words, previous research has predominantly focused on terahertz frequencies and beyond, with limited studies conducted in the visible spectrum. In cases where research has been carried out in this domain, it has mostly involved basic designs and simple resonator rings. This study specifically designs filters that combine meta-surfaces or wavelength-selective filters within the visible range, distinguishing them from conventional thin-film filters. In this study, a diffraction grating has been employed as a novel and innovative structure in filter design. By integrating it with a metasurface and utilizing liquid crystal for precise tunability within a voltage range of 2 to 4 volts, the response speed of the filter has been significantly enhanced. Moreover, this research, which focuses specifically on the visible spectrum, thoroughly investigates and analyzes the impact of increasing the number of layers on the filter's performance, light transmission, and transmission bandwidth.

3. Research methodology

The primary objective of this study is to investigate the optical performance of a tunable filter based on a metasurface and liquid crystal in the visible to near-infrared (VIS–NIR) spectral range. The focus is on designing and simulating structures whose transmission wavelength can be dynamically tuned by applying an external voltage. The significance of this study arises from the demand for filters with fast response times, high spectral accuracy, and the elimination of mechanical components, which are crucial in applications such as hyperspectral imaging and biosensors. The investigated structures consist of one or two aluminum metal layers deposited on a glass substrate, with the space between them filled with nematic liquid crystal type E7. This combination enables a change in the effective refractive index of the structure under the influence of an applied voltage, resulting in a shift in the filter's transmission spectrum.

3.1 Structure design and boundary conditions

The proposed filter structure consists of a glass substrate with a refractive index of 1.46 and a thickness of 150 nanometers, on top of which a 40-nanometer-thick ITO layer is deposited as a transparent electrode and electrical conductor. Due to its optical and electrical properties, this layer plays an effective role in tuning the optical characteristics of the structure. Next, a one-dimensional grating composed of aluminum strips with a thickness of 90 nanometers is periodically patterned on top of the ITO layer. Aluminum is preferred over copper due to its advantages such as lightweight, corrosion resistance, and lower production cost. The periodic design of the strips with a duty cycle of W = P/2 increases the structure's sensitivity to environmental changes such as refractive index variations or applied voltage, enabling tunable optical performance of the structure at different frequencies. This design is highly effective for tunable optical filters and intelligent optical systems. The schematics of the single-layer and double-layer one-dimensional aluminum grating structures on the glass substrate are shown in Fig. 4 and 5.

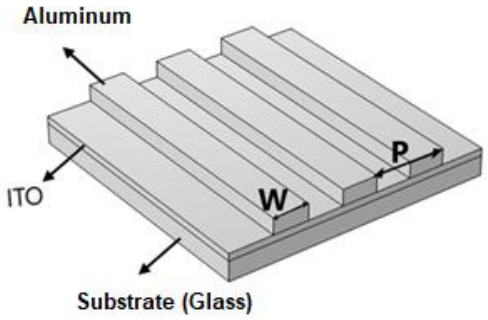


Fig. 4 Schematic of the single-layer one-dimensional aluminum grating structure on a glass substrate

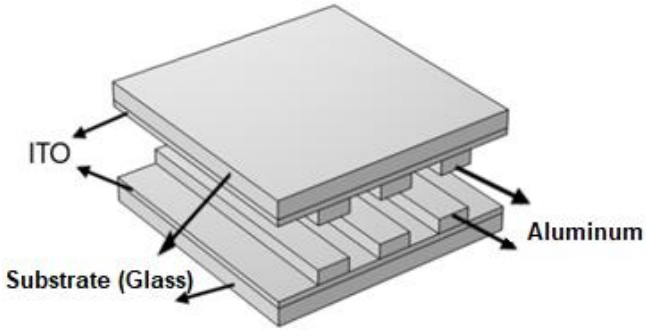


Fig. 5 Schematic of the double-layer one-dimensional aluminum grating structure on a glass substrate

The proposed structure was simulated using COMSOL Multiphysics within the Wave Optics module in a two-dimensional (2D) configuration. In these simulations, the boundary conditions and meshing were defined with high precision to accurately model phenomena such as interference, resonance, reflection, and transmission. The investigation of key parameters such as layer thickness and refractive index, along with the analysis of nonlinear optical phenomena, has led to an accurate modeling of the optical performance of the structure. The two-dimensional simulation enhances both the speed and accuracy of the analyses, enabling the design and optimization of optical structures with targeted functionalities.

3.2 Investigation of the effect of periodicity and light polarization

The influence of periodicity (P) and the polarization state of the incident light (TE and TM modes) on the spectral performance of the filter was analyzed.

- Effect of Periodicity: Various periodicities (300, 400, and 460 nanometers) were applied, and it was observed that increasing the periodicity leads to a red shift in the resonance wavelengths. This phenomenon is attributed to the increased effective propagation path length of the wave within the structure.
- Effect of Polarization: In the TM polarization mode (magnetic field parallel to the surface), resonance modes appeared with higher sharpness and quality compared to the TE mode (electric field parallel to the surface). Moreover, the transmitted light intensity was greater in the TM mode, which is particularly significant for applications requiring high spectral precision.

3.3 Analysis of liquid crystal effect and tunability

In this study, the transmission spectrum of the filter structure was examined under various polarization conditions (TE and TM) and three different periodicities (P) in both single-layer and double-layer configurations. Initially, the base structure was simulated without the presence of liquid crystal to determine its optical response under different conditions. Subsequently, by incorporating the liquid crystal into the structure, the effect of its presence on the transmission characteristics of the filter was analyzed and compared. In the final section, the design of a tunable optical filter using the electro-optic properties of liquid crystal was investigated. In this design, without altering the geometric parameters, spectral tunability was achieved solely by applying voltage, which induces a change in the refractive index of the liquid crystal. The main objective was to evaluate the controllability of the filter's performance with respect to voltage variations and to examine its dependence on polarization type and periodicity.

4. Results and findings

In this section, the transmission spectra of the designed filter are first analyzed under two polarization modes: TE and TM. Subsequently, by adding a second layer to the filter, the transmission performance of the double-layer configuration is compared to that of the single-layer structure (Fig. 6).

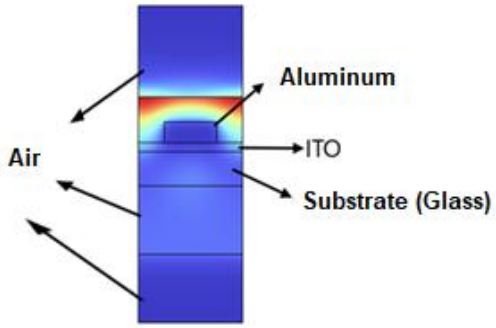


Figure 6: Schematic of the Single-Layer Filter Structure without Liquid Crystal

4.1 Transmission spectrum of the single-layer filter (Aluminum)

The simulated and measured transmission spectra of the single-layer filter without liquid crystal are presented in Fig. 7 for three different grating periods of the aluminum network (P = 300 nm, P = 400 nm, P = 460 nm) under TE and TM polarizations.

Fig. 7(a). In the first graph (P = 300 nm), a sharp dip is observed near 500 nm. In the second graph (P = 400 nm), this dip shifts to a longer wavelength, and an additional peak appears around 450 nm. In the third graph (P = 460 nm), the pattern becomes more complex with multiple dips and peaks visible. As P increases, the range of wavelengths with high transmission changes, and distinct passbands and stopbands emerge. Consequently, the increase in spacing between the structural elements (P) leads to shifts in both the position and intensity of the transmission dips. The structure with P = 460 nm exhibits a more complex behavior, which may be attributed to additional interference effects. These results indicate that by tuning the parameter P, it is possible to shift the wavelengths at which optimal absorption or transmission occurs, which is crucial for the design of optical filters.

For TE polarization (Fig. 7(b)), in the first graph (P = 300 nm), the transmission is significantly low, with a maximum of about 0.2 (20%). A small transmission peak appears near 420 nm, but afterward, the transmission decreases and approaches zero at longer wavelengths. This behavior indicates that, under TE polarization, the structure exhibits lower transmission efficiency compared to the TM mode, blocking or reflecting most of the incident light in the visible range. This indicates that for this value of P, the structure acts almost as a strong absorber or reflector. In the second graph (P = 400 nm), the transmission reaches a maximum of about 0.5 (50%). Two strong peaks appear around 490 nm and 540 nm. A sharp drop in transmission is observed near 490 nm, which is likely due to a strong resonance within the structure. In the third graph (P = 460 nm), two strong peaks similar to those in P = 400 nm are observed, but their positions have slightly shifted toward longer wavelengths. The transmission has increased slightly, yet it still remains below 0.5.

Overall, at P = 300 nm, the structure primarily acts as an absorber, while at P = 400 nm and P = 460 nm, wavelength-selective filtering is observed. The spectral shift (redshift) with increasing P indicates that this parameter can be used to tune the spectral passband and stopband locations.

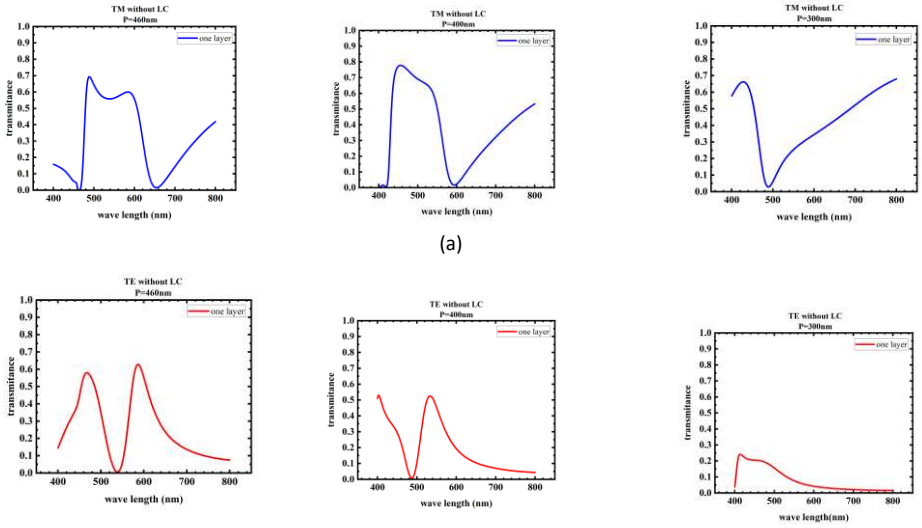


Fig. 7 Simulated and Measured Transmission Spectrum for the Single-Layer Structure at Three Periods (P = 300 nm, P = 400 nm, P = 460 nm) under Polarizations: (a) TM and (b) TE

4.2 Transmission spectra of the filter in the double-layer configuration

The simulated and measured transmission spectra of the filter without liquid crystal in the double-layer configuration for three grating periods (P = 300 nm, P = 400 nm, P = 460 nm) of the aluminum nanostructure under TE and TM polarizations are plotted in Fig. 8.

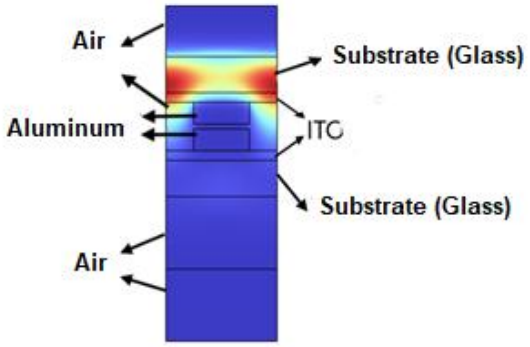


Fig. 8: Schematic of the Double-Layer Filter Structure without Liquid Crystal

In the double-layer configuration for TM polarization (Fig. 9(a)), in the first graph (P = 300 nm), the light transmission is very low, with a maximum of about 0.2 (20%). Two small dips are observed near 440 nm and 490 nm. A gradual increase in transmission is seen beyond 650 nm. At this period, the double-layer structure causes an overall reduction in transmission and creates several small dips. In the second graph (P = 400 nm), the transmission is also very low (less than 15%). Several narrow dips are observed, especially at wavelengths of 450 nm, 490 nm, and 580 nm. Compared to P = 300 nm, the dips have become sharper and their positions have slightly shifted. This period strongly restricts light transmission, turning the structure into a more effective filter. In the third graph (P = 460 nm), we observe a slight increase in transmission (up to 45%). Additionally, several distinct dips appear at 460 nm, 540 nm, and 600 nm. However, these dips are less pronounced compared to those at P = 400 nm. At this period, some of the dips have diminished compared to P = 400 nm, but the transmission remains significantly lower than in the single-layer case. Therefore, adding an additional layer causes a substantial reduction in light transmission. Moreover, increasing the period (P) shifts the positions of spectral dips and increases the complexity of the transmission spectrum. If the goal is higher absorption, the double-layer structure is a better option in the TM polarization.

At this period, some of the dips have diminished compared to P = 400 nm, but the transmission remains significantly lower than in the single-layer case. Therefore, adding an additional layer causes a substantial reduction in light transmission. Moreover, increasing the period (P) shifts the positions of spectral dips and increases the complexity of the transmission spectrum. If the goal is higher absorption, the double-layer structure is a better option in the TM polarization. The first peak exhibits a very high transmission (about 70%), while the second peak is weaker (around 30%). This period results in a filter with two passbands, and compared to P = 300 nm, the transmission intensity has increased. In the third graph (P = 460 nm), two peaks appear around 480 nm and 600 nm. Compared to P = 400 nm, the peaks have slightly shifted in position and their intensities have decreased. This period also creates two passbands, but the transmission intensity has decreased compared to P = 400 nm. In the double-layer structure, the overall transmission increases, resulting in stronger and broader peaks. Additionally, increasing the number of layers improves the filter's performance in terms of light transmission for TE polarization. The best performance is observed at P = 400 nm, where the greatest increase in transmission occurs in the double-layer configuration. These results indicate that using a double-layer structure can enhance the filter's performance and provide better functionality for optical bandpass filters.

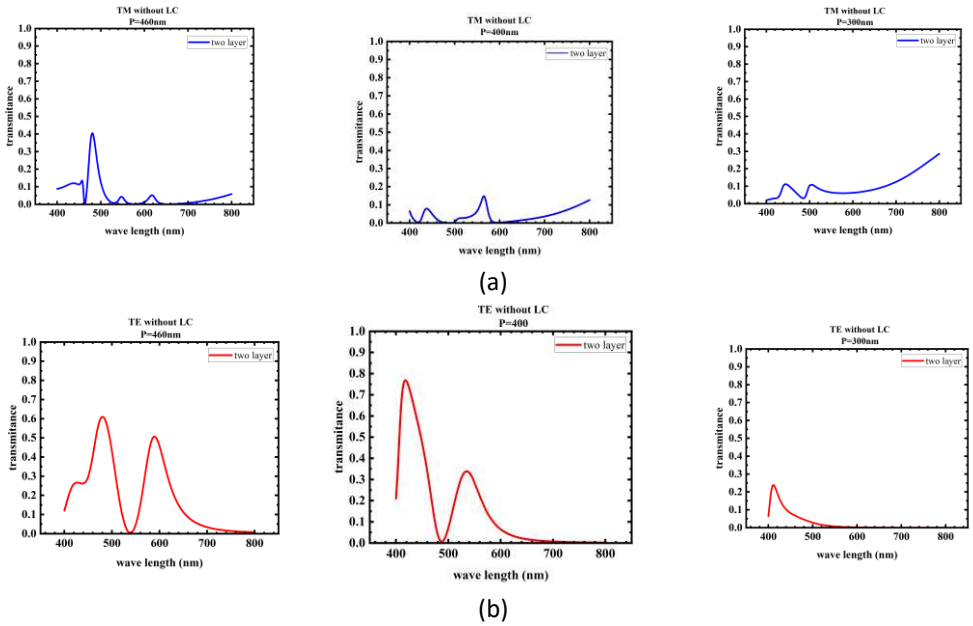


Fig. 9. Simulated and measured transmission spectra for the double-layer configuration at three periods (P = 300 nm, P = 400 nm, P = 460 nm) and polarizations (a) TM and (b) TE.

The following provides a summary of the analyzed cases for both single-layer and double-layer structures under TE and TM polarizations (Table. 1):

Table. 1 Comparison of single-layer and double-layer modes for both polarizations (TE and TM)

Feature	Single-layer (TE)	Double-layer (TE)	Single-layer (TM)	Double-layer (TM)
Overall Transmission	Relatively high (up to 50%)	Higher (up to 70%)	High (up to 80%)	Low (less than 45%)
Transmission Spectrum	Distinct but fewer peaks	Stronger and more diverse peaks	Fewer and broader dips of Strong peaks with broad bandwidths	Multiple and narrower dips, weaker peaks with narrower bandwidths compared to the single-layer
Effect of Changing P	Shift in position and number of peaks	Broader and tunable passbands	Redshift of dips	Decrease in overall transmission and spectral complexity
Suggested Application	Simple narrow-bandpass filter	Broader and tunable bandpass filter	Semi-transparent filter	Stronger absorption filter

Overall, the results obtained from the analysis of single-layer and double-layer structures indicate that the TE polarization performs more favorably than the TM polarization in terms of enhancing light transmission and improving filtering characteristics. In the double-layer structure, TE polarization has achieved stronger transmission peaks and broader passbands, whereas in TM polarization, the overall light transmission is lower and has significantly decreased with the addition of the second layer. Among the investigated periodicities, the structure with P = 400 nm under TE polarization exhibits the best performance, resulting in the highest enhancement in transmission in the double-layer configuration. Therefore, if the objective is to achieve optical filters with high transmission, well-defined, and tunable passbands, employing a double-layer structure under TE polarization would be a more suitable

choice compared to TM polarization. These findings can significantly contribute to the advanced design of optical filters for optoelectronic and photonic applications.

4.3 Analysis of the transmission spectra of the designed filter after liquid crystal integration

In this section, the transmission spectra of the designed filter are analyzed for both TE and TM polarizations. The nematic liquid crystal used in this structure is of the E7 type. For TE polarization, the molecular axis of the liquid crystal is aligned parallel to the electric field direction, and the refractive index of the liquid crystal is ne=1.75. For TM polarization, the electric field is perpendicular to the molecular axis, with a refractive index of no=1.52. As mentioned in Section 1, the effective refractive index of the liquid crystal is calculated using Eq. (1).

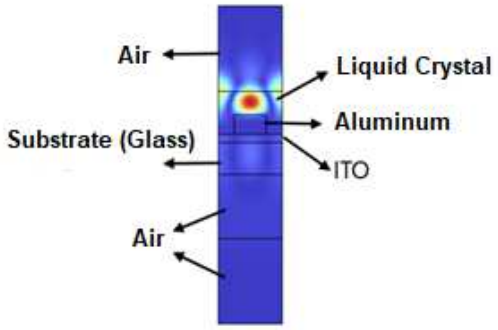


Fig. 10: Schematic of the liquid crystal filter structure in the single-layer configuration

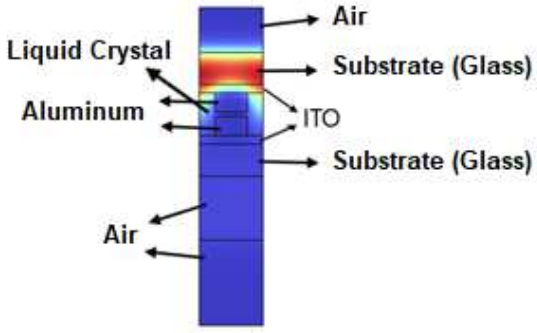


Fig. 11: Schematic of the liquid crystal filter structure in the double-layer configuration

4.4 Transmission spectra of the filter for TM polarization

The transmission spectra of the filter considering the liquid crystal in both single-layer and double-layer configurations for three periods (P=300nm, P=400nm, P=460nm) of the aluminum grid under TM polarization are shown in Fig. 12. As the results indicate, adding the liquid crystal to the structure causes significant changes in the spectral transmission pattern. In all graphs, a notable shift in the positions of resonance peaks is observed, which reflects a change in the effective refractive index and consequently alters the resonance mode conditions of the structure. These shifts can result from the modification of interference conditions and the reconfiguration of the electromagnetic field within the structure. Additionally, the intensity of some resonance peaks has changed compared to the case without the liquid crystal, which may be due to alterations in the coupling conditions between the electric field and the structure, as well as the direct effect of the liquid crystal's refractive index on the behavior of the light wave inside the structure. These results highlight the key role of the liquid crystal in precisely tuning the spectral response and enhancing the tunability of optical filters.

In the comparison between single-layer and double-layer structures across all three periods (P = 300 nm, P = 400 nm, P = 460 nm), significant changes in the transmission pattern are observed. At certain wavelengths, transmission decreases in the double-layer structure, while at others, an increase in transmission is seen. These variations arise from the formation of additional modes and interference effects caused by the presence of the second layer and the liquid crystal, which alter the resonant characteristics of the structure. Notably, in specific regions such as the 600–700 nm wavelength range for P = 400 nm and P = 460 nm, new modes appear in the double-layer structure that are absent in the single-layer one. For the period P=300 nm, the main peak around 438 nm in the single-layer case is significantly stronger than in the double-layer case, indicating a destructive effect of the second layer in this spectral region. For the periods P=400 nm and P=460 nm, notable changes in both the position and intensity of the peaks are observed between the two structures, clearly reflecting the more complex interaction of resonant modes in the double-layer structure for these period values. These results suggest that employing a double-layer structure enables finer tuning of the resonant characteristics and enhances the performance of optical filters within specific spectral ranges.

By examining the effect of the period P on the transmission spectrum, it is observed that with increasing P, the number and positions of resonant peaks in the transmission spectrum change. For P=300 nm, there is a strong resonant peak around 438 nm, where the structure behavior results in only a single main peak in this range. However, for higher periods such as P=400 nm and P=460 nm, multiple peaks appear over a broader wavelength range, indicating greater structural complexity and the influence of additional resonant modes. These changes in the position and number of peaks clearly indicate that with increasing PP, the peaks shift toward longer wavelengths (redshift). This phenomenon results from the change in the lattice spacing and the more complex interactions among resonant modes that intensify as PP increases. This shift toward longer wavelengths, which naturally occurs with increasing period, is due to variations in the effective refractive index and enhanced interference effects within the structure. Such behavior is highly significant for designing optical filters with tunable features and sensitivity to specific wavelengths.

In general, the changes induced by the presence of the liquid crystal are due to the modification of the effective refractive index of the medium. As a material with unique optical properties, the liquid crystal alters the way light interacts with the structure. This change in the effective refractive index causes the resonant modes to shift toward longer wavelengths (redshift). Additionally, the intensity of some resonant peaks either increases or decreases, indicating a change in the coupling conditions of light with the structure. In other words, the liquid crystal significantly affects the energy transmission of light and the interactions of resonant modes. In the double-layer structure, these changes are even more pronounced because the liquid crystal is positioned between the two layers, which enhances its influence on the optical modes. The second layer and the presence of the liquid crystal between the layers cause additional modifications in the transmission pattern, due to the creation of extra modes and interference effects introduced by the second layer. These effects can play an important role in the design of advanced optical filters that require precise tuning of spectral characteristics.

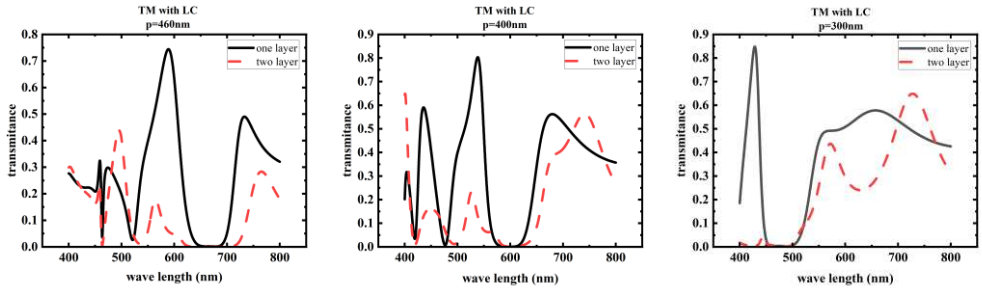


Fig. 12: Simulated and measured transmission spectra for single-layer and double-layer configurations considering liquid crystal at three periods (P = 300 nm, P = 400 nm, P = 460 nm) in TM polarization.

4.5 Transmission spectra of the filter for TE polarization

In Fig. 13, the transmission spectra of the filter with liquid crystal in both single-layer and double-layer configurations are analyzed for three periods (P = 300 nm, 400 nm, 460 nm) under TE polarization. The presence of the liquid crystal significantly affects the position and intensity of the transmission peaks; especially in the double-layer case, where in addition to the shift of the peaks, new resonant modes also emerge. Increasing the period causes the peaks to shift toward longer wavelengths (redshift). The double-layer structure, by creating coupling of additional modes, leads to an increase in light transmission in some regions and a decrease in others. At shorter wavelengths, the double-layer shows lower transmission compared to the single-layer due to new resonances and higher absorption, while at longer wavelengths, transmission increases because of new propagation pathways and constructive resonances. The addition of the second layer causes peak shifts, splitting of peaks, and improvement in light transmission characteristics. Period analysis shows that with increasing P, the resonance peaks shift to longer wavelengths. Overall, the presence of the liquid crystal and the second layer leads to better tunability and enhanced filter performance in TE polarization; the peak bandwidths decrease while the filter efficiency increases. These changes are especially noticeable at longer wavelengths as a redshift. The double-layer structure with liquid crystal offers better optical performance and improves the precision of tuning resonance wavelengths.

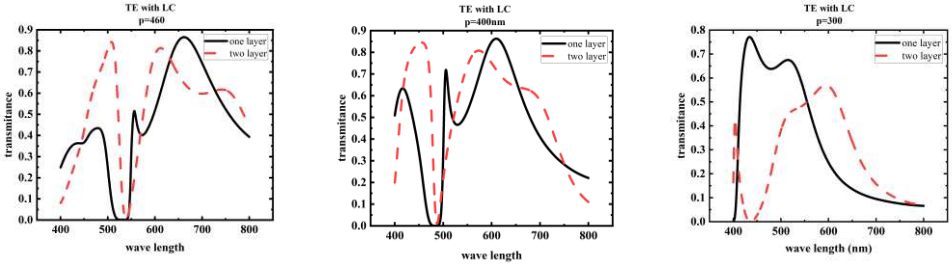


Fig. 13: Simulated and measured transmission spectra for single-layer and double-layer structures considering the liquid crystal at three periods (P=300nm, P=400nm, P=460nm) in TE polarization.

4.6 Analysis of transmission spectrum changes of the designed filter after applying voltage

Fig. 14 shows the changes in the transmission spectrum of the filter as the voltage increases up to 4 volts, after which no significant changes are observed. In the zero-voltage state, the liquid crystal molecules are oriented perpendicular to the incident field, and the transmission spectrum resembles that of TM polarization. As the voltage increases up to 4 volts, the molecules rotate toward the direction of the external field, and the transmission spectrum becomes similar to that of TE polarization. These changes are caused by the variation in the effective refractive index and the orientation of the molecules, which lead to shifts and intensity changes in the resonance peaks. This finding demonstrates that by adjusting the voltage, the optical properties of the structure can be dynamically controlled, enabling the creation of a tunable optical filter.

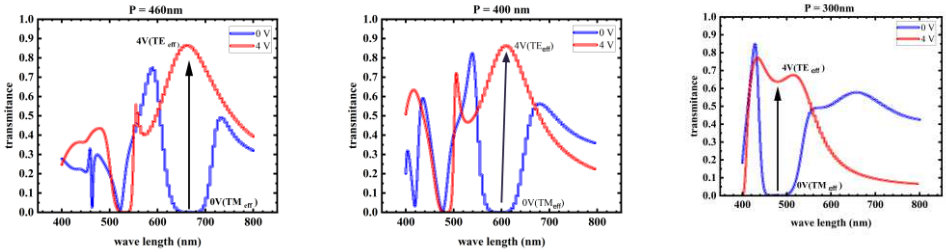


Fig. 14: Measured transmission spectra of the filter for voltages from 0 to 4 volts for three periods (P=300nm, P=400nm, P=460nm).

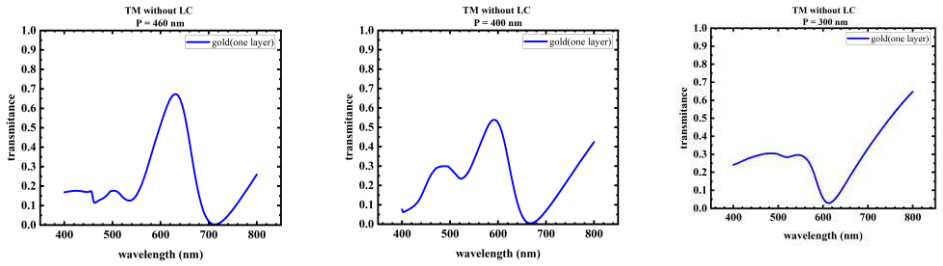
4.7 Transmission spectrum analysis of single-layer gold structures with and without liquid crystal in TE and TM polarizations

The present study provides a detailed analysis of the optical behavior of gold nanoperiodic structures configured as single-layer filters. These structures, with three different periodicities (P = 300 nm, P = 400 nm, and P = 460 nm) and under two polarizations—TE and TM—were experimentally and numerically investigated in two separate conditions: with and without the presence of a liquid crystal. The primary objective of this research is to examine the influence of the geometric periodicity parameter and the role of the liquid crystal on the spectral characteristics of the structure, including the clarity of transmission peaks and the light transmittance within the visible to near-infrared wavelength range.

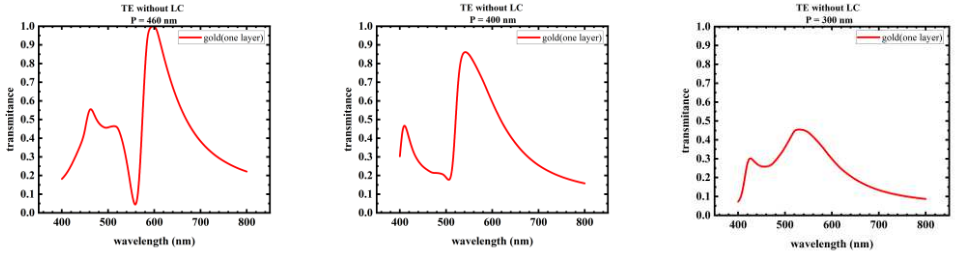
In the first case, where the structure is considered without liquid crystal, the results for TM polarization showed that at a period of 300 nm, the transmission curve exhibited a relatively smooth behavior with only a mild peak around 500 nm having a transmission of approximately 0.3. As the period increased to 400 nm, the spectrum displayed a more oscillatory behavior; specifically, a main resonance peak appeared near 600 nm with a transmission close to 0.55, while a sharp drop occurred at 680 nm, where transmission nearly reached zero. Finally, at a period of 460 nm, the oscillation intensity increases, with a prominent peak appearing at 620 nm and a deep transmission dip reported around 700 nm. These results indicate enhanced coupling of light to the resonant modes of the structure and a spectral response shift towards the red region of the spectrum.

In the TE polarization under the same conditions, it was found that the structure with a 300 nm period lacked prominent resonant peaks, maintaining a maximum transmission of approximately 0.45. At a 400 nm period, a strong resonant peak appeared around 550 nm with a transmission close to 0.85, likely attributed to surface plasmon resonance. With the period increased to 460 nm, a very narrow and intense peak emerges around 590 nm, with its transmission approaching unity. This behavior indicates high spectral resolution and suggests the possible presence of phenomena such as Fano modes or quantum interference within the structure (Fig. 15).

The summary of this section indicates that increasing the structure's period enhances resonant effects, amplifies the amplitude of transmission spectrum oscillations, and shifts the peaks toward longer wavelengths. These characteristics make such structures highly effective for applications like precise optical filters, sensitive optical sensors, and spectral tuners. Conversely, structures with smaller periods, due to their more uniform spectral response, are better suited for systems requiring stable transmission over a broad range.



(a)



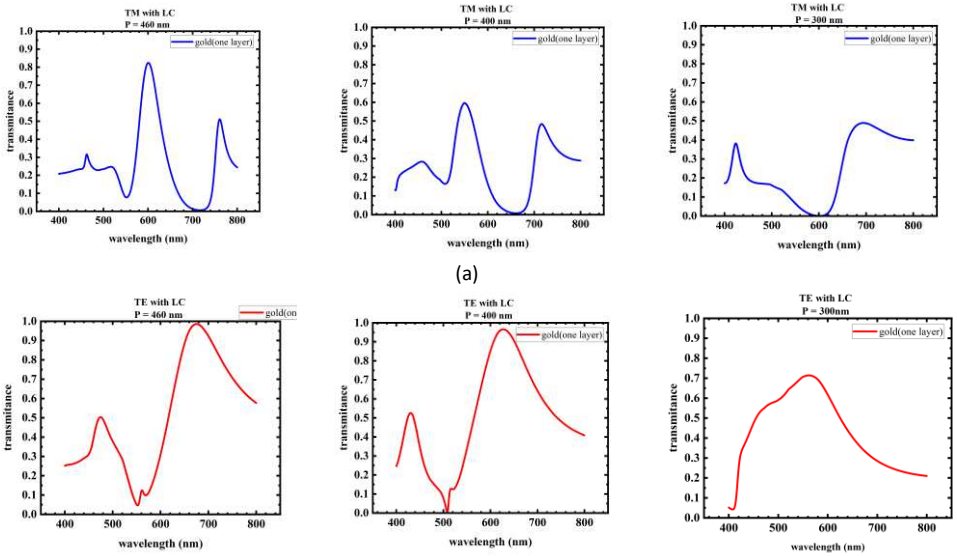
(b)

Fig. 15 Simulated and Measured Transmission Spectrum for the Single-Layer Structure at Three Periods (P = 300 nm, P = 400 nm, P = 460 nm) under Polarizations: (a) TM and (b) TE

In the second part of the study, where the liquid crystal was incorporated into the structure, the optical behavior became significantly more complex and enriched. For TM polarization at a period of 300 nm, an initial resonance peak appeared at 430 nm with an intensity of approximately 0.38, followed by a sharp transmission dip near 600 nm. Increasing the period to 400 nm revealed three distinct peaks at 460, 570, and 710 nm, with the middle peak exhibiting the highest intensity (~0.6). Additionally, a pronounced transmission dip was observed at 650 nm. Finally, at a period of 460 nm, the dominant peak appeared at 630 nm with an intensity exceeding 0.8, accompanied by enhanced spectral clarity and a shift of the peaks toward longer wavelengths. These results indicate improved coupling between the optical modes and the metamaterial structure in the presence of the liquid crystal.

Significant spectral changes were also observed in TE polarization with the inclusion of the liquid crystal. At a period of 300 nm, the transmission spectrum was relatively simple and lacked prominent peaks, with a maximum transmission of about 0.7 at a wavelength of 550 nm. For the 400 nm period, a sharp dip occurred around 500 nm, immediately followed by a strong peak with nearly unity intensity at 600 nm. Increasing the period to 460 nm repeated this pattern, but with the peak shifted to 680 nm and an increased intensity, indicating the direct influence of the period on the position and strength of the resonance peaks (Fig. 16).

The results from this section indicate that the presence of the liquid crystal leads to an increase in the number, clarity, and intensity of resonance peaks, overall enhancement of transmission, and improved structural matching with optical modes. Furthermore, increasing the period in the presence of the liquid crystal results in narrower peak widths, higher spectral resolution, and consequently, enhanced optical performance of the structure.



(a)

(b)

Fig. 16 Simulated and Measured Transmission Spectrum for the Single-Layer Structure at Three Periods (P = 300 nm, P = 400 nm, P = 460 nm) under Polarizations: (a) TM and (b) TE

In summary, it can be concluded that both increasing the structural period and incorporating liquid crystals, independently and synergistically, enhance the intensity and clarity of resonance responses, cause a redshift of spectral peaks, and broaden the optical response range of the structure. Structures with a 460 nm period, particularly in the presence of liquid crystals, demonstrated optimal optical performance. These characteristics make the design of gold nanoperiodic structures a flexible and engineerable tool for the development of advanced optical systems, including precise spectral filters, optical sensors, optical waveguides, and sophisticated optoelectronic devices. Among these, the period parameter plays a crucial role as a key factor in metamaterial engineering, significantly contributing to the optimization and control of optical device performance.

5. Conclusion

In this study, the optical behavior of filters based on single-layer and double-layer nanophotonic structures, consisting of metallic grids with various periods (300, 400, and 460 nm) under both TE and TM polarizations, was thoroughly analyzed and simulated. The results demonstrated that variations in the period and polarization type significantly affect the position, intensity, and number of resonance modes in the transmission spectrum. In TM polarization, the structure with the smaller period (300 nm) exhibited more limited optical transmission and notable dips in the transmission spectrum. This behavior is attributed to the strong interaction of light with the periodic structure and the formation of pronounced resonance modes. Increasing the period to 460 nm resulted in a richer transmission spectrum with more distinct passbands and stopbands, indicating the structure's capability to support multiple optical modes and enhanced tunability of the filter within the studied wavelength range. A similar trend was observed in TE polarization, where increasing the period led to an increase in transmission and a red-shift of the resonance peaks. This effect is attributed to changes in the effective thickness and the boundary conditions for electromagnetic wave propagation. The study of bilayer structures showed that increasing the number of layers results in a more complex spectral response and variations in the intensity of the resonance modes. Particularly in TM polarization, bilayer structures exhibited lower transmission compared to single-layer ones and produced resonance modes with higher resolution. The 400 nm period in the bilayer structure exhibited more distinct passbands and stopbands, resulting in improved filtering performance. In TE polarization, the bilayer structure also produced multiple separate passbands with stronger resonance peaks, significantly enhancing spectral resolution.

The use of E7 liquid crystal as an active material with a tunable refractive index led to an increase in the effective refractive index of the structure and caused the resonance peaks to shift toward longer wavelengths (red shift). This effect was more pronounced in bilayer structures and resulted in the emergence of new modes in the spectrum, originating from optical interference between the layers and changes in the boundary conditions for wave propagation. Moreover, the application of an external electric voltage to the liquid crystal caused reorientation of its molecules and consequently altered the refractive index distribution within the structure. This resulted in dynamic changes in the transmission spectrum and shifts of the resonance peaks. The stabilization of the transmission spectrum after applying 4 volts demonstrated the capability for precise and real-time control of the optical filter characteristics. This feature offers significant potential for applications in active and tunable photonic systems, including sensors, optical switches, and nanophotonic displays.

In conclusion, this study demonstrated that employing bilayer structures and active materials such as liquid crystals enable the design of nanophotonic filters with optimized performance, dynamic tunability, and precise control over the transmission spectrum. These

features are of great importance for the development of advanced and intelligent photonic systems.

Funding Declaration

No funding has been provided for the research.

Data availability

Not applicable.

References

1. J.-F. Lv et al., "Tunable liquid crystal metamaterial filter with polarization-insensitive characteristic," Liquid Crystals, vol. 49, no. 10, pp. 1338-1346, 2022.
2. Z.-W. Xie, J.-H. Yang, V. Vashistha, W. Lee, and K.-P. Chen, "Liquid-crystal tunable color filters based on aluminum meta-surfaces," Optics express, vol. 25, no. 24, pp. 30764-30770, 2017.
3. "Surface Plasmon Resonance basics." chrome-extension://efaidnbmnnnibpcajpcglclefindmkaj/https://glaserr.missouri.edu/vitpub/teaching/3700s13/SP13A04_SPR.pdf (accessed.
4. D. Remler and A. Haymet, "Phase transitions in nematic liquid crystals: a mean-field theory of the isotropic, uniaxial, and biaxial phases," The Journal of Physical Chemistry, vol. 90, no. 21, pp. 5426-5430, 1986.
5. G. Si, Y. Zhao, E. S. P. Leong, and Y. J. Liu, "Liquid-crystal-enabled active plasmonics: a review," Materials, vol. 7, no. 2, pp. 1296-1317, 2014.
6. J. Beeckman, D. P. Medialdea, T. Hui, K. Neyts, and X. Quintana, "Fast visible-near infrared switchable liquid crystal filter," Molecular Crystals and Liquid Crystals, vol. 502, no. 1, pp. 9-18, 2009.
7. T. Yuan et al., "Tunable-liquid-crystal-filter-based low-light-level color night vision system and its image processing method," Applied Optics, vol. 58, no. 18, pp. 4947-4955, 2019.
8. S. P. Palto et al., "Voltage-tunable optical transmission of subwavelength metal gratings filled with liquid crystals," in Metamaterials X, 2016, vol. 9883: SPIE, pp. 21-28.
9. P. Bahlouli and A. Chaharmahali, "Design and Simulation of a Bandpass Filter Using Microstrip Lines for Application in Low Noise Amplifier Design," presented at the 2nd National Conference on Knowledge and Technology in Electrical, Computer and Mechanical Engineering of Iran, 2018. [Online]. Available: https://civilica.com/doc/784066
10. "Design and Simulation of an Electrically Tunable Optical Filter Based on Ring Resonators," M.S. thesis, Faculty of Engineering, University of Bonab, Ministry of Science, Research and Technology, Iran, 2015.
11. Q. Cao and P. Lalanne, "Negative role of surface plasmons in the transmission of metallic gratings with very narrow slits," Physical Review Letters, vol. 88, no. 5, p. 057403, 2002.
12. B. Yu et al., "Liquid Crystal Enables Extraordinarily Precise Tunability for a High-Q Ultra-Narrowband Filter Based on a Quasi-BIC Metasurface," Advanced Functional Materials, vol. 35, no. 2, p. 2413098, 2025.
13. C. Shen, J. Sun, Y. Qi, S. Lv, and S. Wei, "Electrically tunable all-dielectric meta-surfaces integrated with nematic liquid crystals for information encryption," IEEE Photonics Journal, vol. 13, no. 4, pp. 1-5, 2021.
14. G. Mirbagheri and D. T. Crouse, "Design, fabrication, and spectral characterization of temperature-dependent liquid crystal-based metamaterial to tune dielectric metasurface resonances," in Terahertz, RF, Millimeter, and Submillimeter-Wave Technology and Applications XV, 2022, vol. 12000: SPIE, pp. 115-125.